Sedimentary Geology 238 (2011) 268–276

Contents lists available at ScienceDirect

Sedimentary Geology

journal homepage: www.elsevier.com/locate/sedgeo

Laboratory evaluation of two LISST-25X using river sediments

Leonardo Filippa [a,*], Luana Freire [b], Alfredo Trento [a], Ana M. Álvarez [a], Marcos Gallo [b], Susana Vinzón [b]

[a] Facultad de Ingeniería y Ciencias Hídricas, Universidad Nacional del Litoral (FICH-UNL), CC 217, (3000) Santa Fe, Argentina
[b] Área de Engenharia Costeira e Oceanográfica, Programa de Engenharia Oceânica (PEnO)/COPPE, Universidade Federal do Rio de Janeiro (UFRJ), CT C-209 Cx Po 68508-21945-970 Rio de Janeiro, RJ, Brazil

ARTICLE INFO

Article history:
Received 4 October 2010
Received in revised form 15 April 2011
Accepted 27 April 2011
Available online 6 May 2011

Editor: G.J. Weltje

Keywords:
LISST-25X
Sauter Mean Diameter (*SMD*)
Sediments
Granulometric distribution

ABSTRACT

There are different methods to determine particle size, most of them are only applicable in the laboratory. In order to describe the suspended fine sediment sizes where flocs may be part of the suspension, in situ measurements are essential. This work shows the results of sediment size measurements done in the laboratory using two LISST-25X diffractometers, developed for in-situ measurements, and a Malvern Mastersizer 2000 diffractometer for laboratory use. The two LISST-25X models characterize the sample size through the Sauter Mean Diameter (*SMD*). Besides the *SMD*, the Malvern diffractometer determines the granulometric distributions of the samples.

The tested samples are from different fluvial and estuarine environments (Paraná, Salado and the Amazon Rivers) and their sizes (*SMD*) range from 4 to 300 μm.

The relationship between *SMD* obtained with the two LISST-25X and the Malvern diffractometers gave a determination coefficient of $R^2 = 0.98$. Compared to the Malvern instrument, used as a reference, it was observed that the LISST instruments tend to overestimate the measured *SMD* for diameters lower than 20 μm, and to underestimate the values of samples with larger diameters (>20 μm). Aiming to obtain other characteristic diameters of the granulometric distribution from *SMD* measurements obtained with LISST-25X diffractometers, correlations between *SMD* and d_{10}, d_{50} and d_{90}, were established. The dependency of the measurement of sediment mass concentration obtained with LISST instruments, with the particle size, is also addressed.

1. Introduction

Different methods have been developed to determine particle size (Rawle, 2010), most of them are only applicable under laboratory conditions. However, for the size characterization of suspended fine sediments with formation or presence of flocs, in situ measurements are essential. The instruments available for field particle measurements include, among others, the series of LISST (Laser In-Situ Scattering and Transmissometry) sensors: LISST-25X, LISST-100, LISST-SL and LISST-ST, Sequoia Scientific Inc. Few comparisons between in situ laser diffraction methods and other techniques are available in the literature. For instance, Eisma et al. (1996) used a Malvern field-adapted instrument deployed along with submersible video and photographic devices. It was found that Malvern underestimates sizes when compared to the other devices, due to its tendency to break the aggregates. A comparison between LISST-100 and acoustical and optical sensors made by Lynch et al. (1993) showed positive correlations between the LISST and the other instruments. Stramski (2006) also compared LISST-100 and a photographic sensor. It was found that LISST-100 is more accurate than the photographic sensor particularly for measuring small particles, because of sensor resolution limitations. The main limitation of LISST-100 mentioned in those works is the lack of accuracy when the particle size reaches the detection limits of the instrument.

Agrawal and Pottsmith (1994), Traykovski et al. (1999), Gartner et al. (2001), Agrawal et al. (2008), among others, report field and laboratory projects with more advanced equipment, LISST-100 and LISST-ST. With regard to LISST-25X, used in this project, Agrawal and Mikkelsen (2009) explained the operating principle of the equipment, and Topping et al. (2006) used this instrument to determine suspended sediment concentrations and sediment sizes in a reach of Colorado River (USA).

The operating principle of the LISST-25X instrument is based on a low angle laser light scattering proposed by Lorenz–Mie (Sequoia, 2008). According to this principle, the small particles scatter most light at big angles, whereas big particles scatter light at very small angles. The LISST-25X instrument determines the Sauter Mean Diameter of the complete sample (*SMD*), the Sauter Mean Diameter of the coarse fraction, >63 μm (SMD_g), the total suspended sediment volume concentration (*SSC*), the coarse suspended sediment volume concentration (SSC_g), the optical transmission level (*OT*), and the instrument operating depth.

The *SMD* (also called d_{32} or $D[3,2]$) is used to characterize the sizes of the suspended sediment. It is defined as the diameter of a sphere

* Corresponding author.
E-mail address: leofi2004@yahoo.com.ar (L. Filippa).

0037-0738/$ – see front matter © 2011 Elsevier B.V. All rights reserved.
doi:10.1016/j.sedgeo.2011.04.017

that has the same volume/surface area ratio as the particle of interest. Mathematically, it is defined according to the following equation (Pacek et al., 1998):

$$SMD = d_{32} = \frac{\int_{d_{min}}^{d_{max}} d^3 p(d)\mathrm{d}d}{\int_{d_{min}}^{d_{max}} d^2 p(d)\mathrm{d}d} \quad (1)$$

where d indicates the particle diameter, d_{max} and d_{min} indicate the maximum and minimum diameters of particle distribution, respectively, and $p(d)$ indicates the probability density function of d. The LISST-25X instrument mathematically transforms the scattering intensity into the following two variables: particle volume concentration, SSC^{vol}, and particle area concentration, SSC^{sup}. It then determines the sample SMD based on the following relationship between the concentrations (Agrawal and Mikkelsen, 2009):

$$SMD = 1.5\frac{SSC^{vol}}{SSC^{sup}}. \quad (2)$$

The coefficient 1.5 results from considering the surface area projected. More detailed information about the operating principle of the LISST-25X sensors as well as an introduction to the equations to calculate the output variables can be found in Agrawal and Mikkelsen (2009).

According to Sequoia Scientific Inc. (Sequoia, 2009), LISST-25X can measure: SMD between 2.50 μm and 500 μm; SMD_g between 63 μm and 500 μm; SSC and SSC_g from 0.10 to 1000 mg/L, approximately, for an optical path length of 2.50 cm; OT varies at the 0–100%, with an optimum interval of 30–98%. The optical path length is the product of the geometric length of the path that the light follows through the system, and the index of refraction of the medium through which it propagates. The SMD and SSC vary linearly according to the optical path length of the instrument. The SMD variation is directly proportional to the path length, whereas for SSC the relation is inverted. The instrument resolution is 0.025% for SSC and SSC_g, 1.0 μm for SMD and SMD_g and 0.10% for OT.

Malvern Mastersizer 2000 is broadly used in laboratory work. There are a variety of applications within Malvern to measure particle sizes, including measuring emulsions, suspensions and dry powders. Some applications for sediment size determinations can be found in Murray and Holtum (1996), Dyer and Manning (1999), Mietta et al. (2009), Manning et al. (2009) and Kumar et al. (2010). Thus, the Malvern measurements will be considered in the following comparisons as a reference device.

The aim of this project was to compare the sediment sizes recorded by two LISST-25X instruments (here called "model 1" and "model 2") with the sediment sizes measured by a Malvern Mastersizer 2000 instrument (Malvern Instruments Ltd.). The in situ devices are meant for floc size measurements. However, due to the uncertainties of creating a uniform suspension and sampling for floc size measurement, the comparison was based on single particle determinations. This comparison aims to highlight the main limitations of the in situ instruments, and their operational conditions regarding the size and concentration ranges.

Different samples of natural sediments collected in fluvial and estuarine environments were used. From this comparison correlations between SMD and diameters widely used in fluvial and maritime engineering, such as d_{50}, were also established.

2. Methodology

The tests were carried out with a LISST-25X optical path length of 2.50 cm (model 1) in FICH/UNL (Argentina) and LISST-25X optical path length of 0.30 cm (model 2) in LDSC/COPPE/UFRJ (Brazil). Both instruments were immersed in an acrylic prismatic testing chamber (14.50 cm × 11.50 cm × 12 cm and a total volume of 1.35 L) provided by the manufacturer, and the equipment was mounted horizontally to avoid particle sedimentation on the sensor (Sequoia, 2009). Fig. 1 shows the experimental set up.

Thirty seven sediment samples with different size distribution and origin were tested: glass micro-spheres Whitehouse Scientific (E), brick dust (B) and sediment samples from the Paraná River, Argentina (PR); the Salado River, Argentina (S), and the Amazon River, Brazil (AM). Sodium hexametaphosphate (13.50 mL, 4%) was added as a dispersant in order to avoid flocculation. The granulometric composition and the SMD of the samples were previously determined by Malvern from the average of three consecutive measurements. The source, the sizes of the samples and the granulometric classification

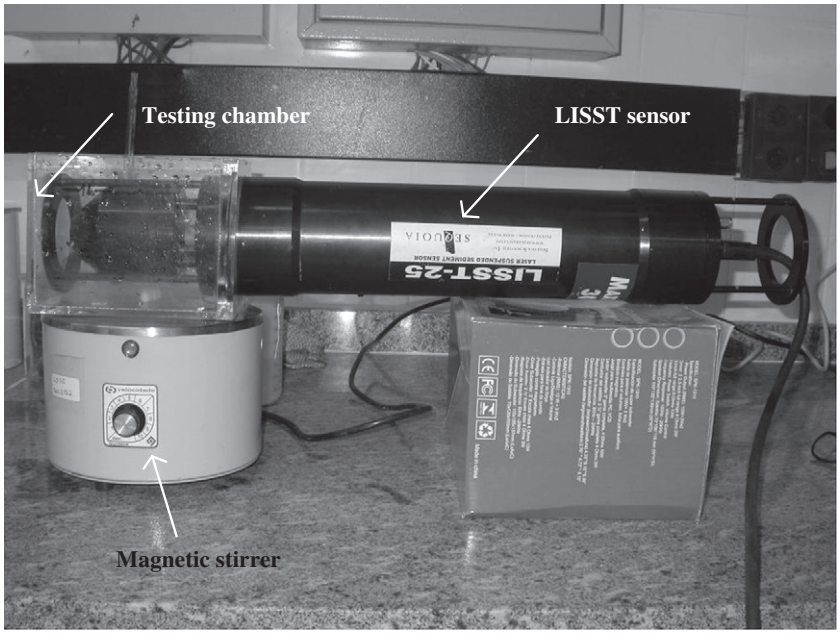

Fig. 1. Experiment set up using LISST-25X (testing chamber and magnetic stirrer).

Table 1
List of tested samples, source and granulometric composition obtained with Malvern Mastersizer. Thick-stroke lines are used to separate the three groups: Group 1, samples with prevalence of fine sediments; Group 2, samples composed of medium and coarse silt particles; Group 3, samples with a higher content of sand.

#	Sample	Source	Clay ϕ<9 (%)	Very fine silt 9<ϕ<7 (%)	Fine silt 7<ϕ<6 (%)	Mean silt 6<ϕ<5 (%)	Coarse silt 5<ϕ<4 (%)	Very fine sand 4<ϕ<3 (%)	Fine to very coarse sand 3<ϕ<2 (%)
1	AMP5H3G1	Suspended sediments, Amazon river mouth	7.4	28.1	21.4	29.4	8.0	5.3	0.4
2	B41	Brick dust (<41.5 μm)	0.9	34.1	24.0	34.4	6.0	0.6	0.0
3	B35	Brick dust (<35 μm)	0.9	34.9	25.8	35.0	3.1	0.3	0.0
4	B49	Brick dust (<49 μm)	0.8	36.4	25.9	30.9	5.0	1.0	0.0
5	B28	Brick dust (<28 μm)	0.9	36.6	27.3	33.2	1.7	0.3	0.0
6	AMP5H1G4	Suspended sediments, Amazon river mouth	9.6	38.9	21.0	12.9	2.4	3.5	11.7
7	B22	Brick dust (<22.5 μm)	1.2	47.3	28.2	19.2	1.5	1.9	0.7
8	B58	Brick dust (<58 μm)	2.2	35.9	26.8	26.7	6.2	2.2	0.0
9	S25b	Suspended sediments, Salado river	3.8	9.7	9.6	23 .2	15.5	22.1	16.1
10	S19F	Suspended sediments, Salado river	3.7	19.7	16.4	32.3	17.1	10.8	0.0
11	AMP5H3G4	Suspended sediments, Amazon river mouth	5.0	17.9	19.5	41.1	9.9	6.4	0.2
12	S25bF	Suspended sediments, Salado river	6.0	13.1	12.8	32.3	21.5	14.3	0.0
13	PRF	Bed sediments, Parana river	1.4	4.6	5.4	25.6	29.2	33.6	0.2
14	S36F	Suspended sediments, Salado river	1.6	13.1	14.7	33.2	21.9	15.4	0.1
15	S37F	Suspended sediments, Salado river	2.2	9.5	9.6	29.7	25.6	23.4	0.0
16	AMP5H1G1	Suspended sediments, Amazon river mouth	4.9	15.3	15.1	41.4	16.8	6. 4	0.1
17	S28bF	Suspended sediments, Salado river	4.9	8.6	9.5	33.2	26.2	17.6	0.0
18	S28aF	Suspended sediments, Salado river	1.2	7.2	7.6	31.5	29.7	22.8	0.0
19	S24CF	Suspended sediments, Salado river	1.7	8.2	9.8	35.5	27.5	17.3	0.0
20	S29F	Suspended sediments, Salado river	1.0	4.7	5.1	32.4	32.8	23.9	0.1
21	E2	Glass (25 to 32 μm)	0.0	0.0	0.0	98.0	2.0	0.0	0.0
22	S29	Suspended sediments, Salado river	0.6	3.1	4.5	24.7	21.1	24.6	21.4
23	S36	Suspended sediments, Salado river	0.8	5.8	7.5	22.7	15.6	26.4	21.2
24	S23	Suspended sediments, Salado river	3.1	4.9	5.3	20.3	16.8	28.7	20.9
25	S28a	Suspended sediments, Salado river	0.6	3.2	4.4	20.9	21.2	35.0	14.7
26	S28b	Suspended sediments, Salado river	0.6	3.3	4.6	20.9	19.3	31.7	1 9.6
27	S37OR	Suspended sediments, Salado river	1.4	6.7	6.1	17.2	15.0	38.1	15.5
28	SP1	Bed sediments, Parana river (75% PR); suspended sediments, Salado river (25 % S37F)	0.6	3.3	3.2	9.9	8.7	10.3	64.0
29	S37G	Suspended sediments, Salado river	0.5	3.5	2.3	5.7	6.8	52.1	29.1
30	AM76	Bed sediments, Amazon tidal flats	0.0	0.0	0.0	0.0	16.4	81.9	1.7
31	SP2	Bed sediments, Parana river; (90 % PR) suspended sediments, Salado river (10% S37F)	0.3	2.1	1.9	5.6	5.0	7.4	77.7
32	AM107	Bed sediments, Amazon tidal flats	0.0	0.8	0.6	2.4	10.7	76.0	9.5
33	AM137	Bed sediments, Amazon tidal flats	0.0	0.7	0.6	1.6	2.5	17.2	77.4
34	AM165	Bed sediments, Amazon tidal flats	0.0	0.1	0.4	1.3	1.3	5.9	91.0
35	AM215	Bed sediments, Amazon tidal flats	0.0	0.0	0.2	0.9	0.7	3.9	94.3
36	PR	Bed sediments, Parana river	0.0	0.0	0.0	0.0	0.0	3.4	96.6
37	E1	Glass (72 to 90 μm)	0.0	0.0	0.0	0.0	0.0	100.0	0.0

Note: The samples labeled with the letter F were previously sieved using an ASTM 230 sieve.

based on the *phi* (ϕ) scale (Shen and Julien, 1993) are presented in Table 1. Fig. 2 shows a comparison of the tested samples.

The samples were classified into three major groups, according to the predominant fractions (see Table 1): Group 1 (sample #1 to #8), with prevalence of fine sediments; Group 2 (sample #9 to #21), composed of medium and coarse silt particles; and Group 3 (sample #22 to #37), samples with a higher content of sand. Fig. 3 shows granulometric cumulative distribution for a typical sample of each group, AMP5H3G1 (Group 1), PRF (Group 2) and S37G (Group 3).

The samples whose measurements were made using LISST instruments were diluted in distilled water filling the testing chamber. During measurements, the water–sediment mixture was stirred continuously using a magnetic stirrer (see Fig. 1). As the coarse particle concentration increased, the mixture was also manually stirred. The sediment samples with high content of coarse material (E1, SP1, SP2, PR, AM137, AM165 and AM215) were gradually dumped on the sensor lenses, according to Traykovski et al. (1999). All tests were performed at constant environment light and temperature (25 °C) conditions, and under homogeneous mixture conditions, avoiding density gradients in the suspension.

In every test, *SMD*, SMD_g, *SSC*, SSC_g and *OT* values were obtained at fixed intervals.

Model 1 was set to make a total of 40 measurements per sample at a sampling rate of 5 s, and model 2 to make a total of 20 measurements per sample at a sampling rate of 2 s. For each sediment sample, the mean values and the *SMD* variation coefficient (*CV*) were determined (*CV* is defined as the ratio between the standard deviation of the *SMD* measurement and the *SMD* mean value). Four samples, E1, E2, B41 and B58, were tested with both LISST equipments (models 1 and 2).

3. Results

3.1. Comparison between SMD obtained with LISST and Malvern instruments

Table 2 summarizes the major results of the tested samples. It shows the corresponding mean sizes (*SMD*, SMD_g), variation coefficients (*CV SMD*) and mean concentration values (*SSC*, SSC_g/*SSC*, *OT*) measured with the LISST-25X instruments, as well as the d_{10}, d_{50}, d_{90} and *SMD* measured with Malvern.

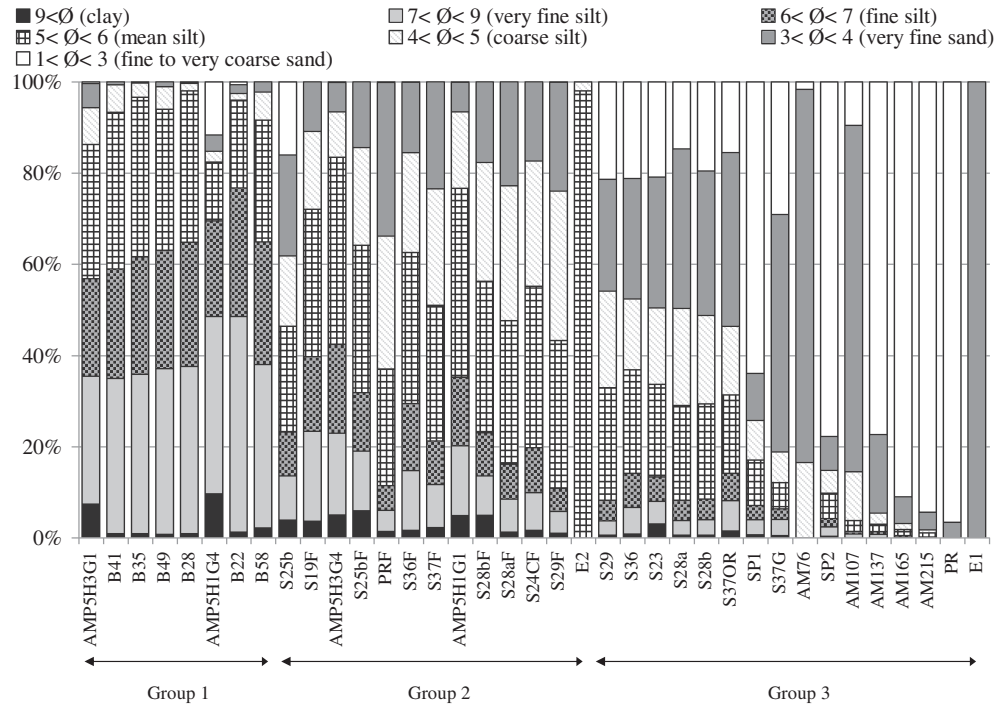

Fig. 2. Granulometric composition of samples obtained with Malvern Mastersizer. Percentages of clay, very fine silt, fine silt, mean silt, coarse silt, very fine sand, fine and coarse sand.

Fig. 4 compares the *SMD* measured using the two LISST-25X sensors to the *SMD* measured with the Malvern diffractometer. The *SMD* ranged from 4 to 300 μm, approximately. The correlation coefficient was $R^2 = 0.98$. The PR sample was excluded from this correlation due to its high sand content (Fig. 2).

From the comparison shown in Fig. 4, it is possible to note that for smaller sizes (*SMD*<20 μm) the diameters measured with LISST tend to be larger than those measured with Malvern. For instance, this was the case with B49, B41, S25bF and S28bF samples (Groups 1 and 2) because they had a high percentage of fine material, 99, 99, 85 and 82%, respectively. The maximum relative difference observed between the measured *SMD* was 80% (5.9 μm, for the S25bF sample). For larger sizes, the *SMD* measured with LISST showed lower results than those measured with Malvern. Belonging to this group (Group 3) are

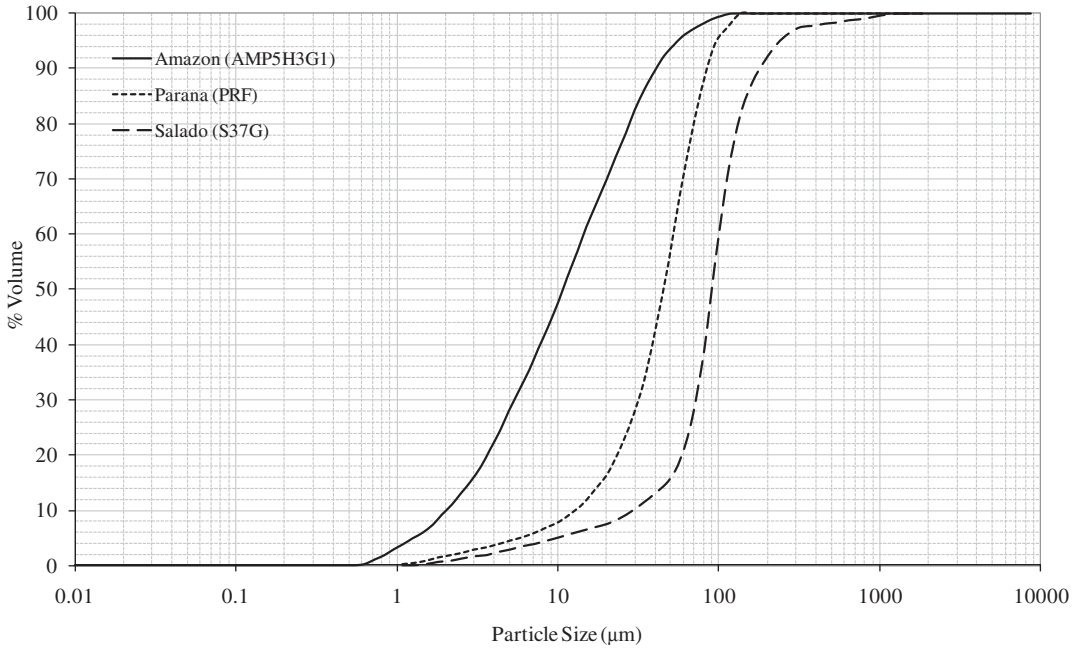

Fig. 3. Granulometric curves corresponding to indicative samples of each subgroup: AMP5H3G1 (Group 1), PRF (Group 2) and S37G (Group 3).

Table 2
List of results using LISST-25X and Malvern Mastersizer: mean sizes (*SMD*, SMD_g), variation coefficients (*CV SMD*), and mean concentration values (*SSC*, SSC_g/SSC, *TO*) measured with the LISST-25X sensors, and d_{10}, d_{50}, d_{90} and *SMD*, measured with Malvern. Models 1 and 2 are identified by optical paths — 2.5 cm and 0.3 cm, respectively. Measured and prepared concentrations are also reported (N/D: no data).

#	Sample	LISST-25X						Malvern Mastersizer					*SSC* (mg/L)	*Source*
		SMD (μm)	*CV SMD*	SMD_g (μm)	*SSC* (mg/L)	SSC_g/SSC	*TO*	*Optical path (cm)*	*SMD* (μm)	d_{10} (μm)	d_{50} (μm)	d_{90} (μm)		
1	AMP5H3G1	6.9	0.1	−17.7	186.6	0.0	0.84	0.3	5.8	2.3	12.3	46.7	N/D	Amazon
2	B41	10.5	0.1	180.9	358.0	0.0	0.79	0.3	7.2	2.7	11.93	35.3	N/D	Brick dust
		9.8	0.0	−15.9	88.2	0.0	0.35	2.5					200	
3	B35	8.5	0.0	103.0	288.3	0.0	0.77	0.3	7.0	2.7	11.39	30.6	N/D	Brick
4	B49	11.2	0.0	−184.8	612.1	0.0	0.70	0.3	6.9	2.7	10.93	33.2	N/D	Brick
5	B28	7.1	0.0	143.0	374.9	0.0	0.63	0.3	6.8	2.6	10.70	27.5	N/D	Brick
6	AMP5H1G4	3.8	0.1	3.0	28.5	0.0	0.98	0.3	4.8	1.9	7.9	167.0	N/D	Amazon
7	B22	6.6	0.0	−70.5	485.6	0.0	0.53	0.3	5.7	2.4	7.89	24.2	N/D	Brick
8	B58	8.7	0.0	8.4	270.8	0.0	0.27	2.5	7.6	2.7	9.8	30.7	200	Brick dust
		8.7	0.0	−235.1	1020.2	0.0	0.49	0.3					N/D	
9	S25b	16.2	0.1	92.7	118.2	0.2	0.75	2.5	10.6	5.6	44.3	172.0	100	Salado
10	S19F	7.8	0.2	4.3	326.0	0.0	0.33	2.5	6.5	2.8	20.3	57.7	200	Salado
11	AMP5H3G4	9.7	0.1	16.8	278.2	0.0	0.83	0.3	7.8	3.3	18.1	50.4	N/D	Amazon
12	S25bF	13.4	0.0	53.5	139.9	0.1	0.68	2.5	7.4	3.6	28.9	69.1	100	Salado
13	PRF	11.3	0.1	−181.5	7.1	0.0	0.98	2.5	12.8	10.8	47.9	87.1	200	Paraná
14	S36F	12.9	0.1	59.1	107.6	0.1	0.71	2.5	13.7	5.8	29.8	70.6	100	Salado
15	S37F	9.3	0.0	24.9	270.7	0.0	0.41	2.5	8.4	4.3	36.6	75.6	200	Salado
16	AMP5H1G1	9.8	0.1	−12.1	173.8	0.0	0.89	0.3	8.4	3.5	23.5	53.7	N/D	Amazon
17	S28bF	14.7	0.0	62.1	263.6	0.1	0.53	2.5	9.1	5.3	35.6	72.9	200	Salado
18	S28aF	16.8	0.0	70.9	256.4	0.1	0.57	2.5	19.0	9.6	41.6	77.2	200	Salado
19	S24CF	9.9	0.0	10.6	282.6	0.0	0.43	2.5	8.9	5.4	34.5	67.3	200	Salado
20	S29F	18.8	0.1	75.4	210.2	0.2	0.65	2.5	22.9	14.8	43.9	79.2	200	Salado
21	E2	26.3	0.1	315.2	94.6	0.1	0.84	2.5	29.0	24.0	29.4	33.6	226	Glass spheres
		30.1	0.0	416.2	196.2	0.0	0.98	0.3					N/D	
22	S29	26.9	0.1	111.1	211.6	0.3	0.72	2.5	31.2	18.4	56.6	347.3	200	Salado
23	S36	16.4	0.1	109.8	191.4	0.3	0.66	2.5	24.2	11.6	57.9	206.5	200	Salado
24	S23	14.1	0.1	93.1	150.7	0.2	0.68	2.5	14.1	11.0	61.0	213.4	100	Salado
25	S28a	20.2	0.1	97.2	172.0	0.3	0.71	2.5	31.3	18.7	61.4	144.7	200	Salado
26	S28b	21.5	0.1	133.3	121.4	0.3	0.79	2.5	31.4	18.2	63.4	201.0	100	Salado
27	S37OR	16.2	0.1	85.9	156.4	0.3	0.69	2.5	12.2	7.4	63.9	148.4	200	Salado
28	SP1	36.8	0.2	233.9	983.4	0.8	0.39	2.5	42.3	23.3	247.8	641.9	N/D	Paraná
29	S37G	33.6	0.1	115.1	89.9	0.7	0.89	2.5	40.3	32.0	90.1	195.9	100	Salado
30	AM76	89.0	0.1	107.5	2787.0	0.8	0.78	0.3	74.4	56.1	76.8	104.2	N/D	Amazon
31	SP2	57.1	0.3	235.2	154.4	0.9	0.89	2.5	66.9	40.7	307.2	659.9	250	Paraná
32	AM107	102.0	0.1	110.3	2682.2	0.8	0.78	0.3	65.3	55.5	84.2	119.4	N/D	Amazon
33	AM137	128.4	0.3	164.2	10299.0	0.9	0.52	0.3	100.5	96.0	151.9	211.7	N/D	Amazon
34	AM165	158.8	0.3	183.3	11964.0	0.9	0.57	0.3	149.3	125.3	192.5	263.2	N/D	Amazon
35	AM215	247.7	0.2	246.2	3158.0	1.0	0.83	0.3	204.7	167.9	250.1	346.3	N/D	Amazon
36	PR	19.0	0.1	292.4	62.5	1.0	0.86	2.5	301.6	175.4	346.3	726.9	N/D	Paraná
37	E1	86.3	0.0	99.4	54.8	0.9	0.96	2.5	81.9	74.1	82.1	91.7	500	Glass spheres
		92.5	0.4	97.2	25.1	1.0	0.98	0.3					N/D	

the S36, S28a, S28b, S37G, SP1 and SP2 samples with high percentages of sand, 48, 49, 51, 81, 74 and 85%, respectively. The maximum difference in this case was −56% (36.7 μm, for the AM107 sample).

For the four samples tested using the two LISST-25X models (B41, B58, E2 and E1) a positive correlation was observed between the resulting *SMD*, with differences of 7% (0.7 μm), 1% (0.1 μm), 14% (3.8 μm) and 7% (6.2 μm), respectively.

The measurements were done within or close (samples PRF, E1 and B58) to the optimum optical transmission (*OT*) levels, from 30% to 98%. When these limits were exceeded the size measurement was not good and thus discarded.

The variability in the *SMD* measurements using LISST instruments was quantified. Fig. 5 shows the *CV* as a function of *SMD*. It is possible to observe that the *CV* increases as the sample *SMD* increases. The minimum and maximum *CV* were 0.02 (B28) and 0.43 (E1), respectively.

Regarding the coarse fraction analysis, given by LISST instruments through SMD_g values, Fig. 6 shows the comparison between the SMD_g and d_{90} (obtained with Malvern), indicating a good consistency in the results. However, as shown in Table 2, SMD_g is calculated even without the presence of coarse particles (see for instance samples in Group 1), when SSC_g equals zero, and consequently SMD_g recordings must be discarded.

3.2. Sediment concentrations measured with LISST instruments

The expected inverse relationship between the *SSC* measurements and the optical transmission level is observed for the tested samples (Table 2). Fig. 7 presents the relationship between the *SSC* measured with LISST and the corresponding sizes, *SMD*, for each suspension concentration (actual *SSC*). For natural sediments, the volume concentrations obtained by LISST (μL/L) were multiplied by the density, 2.65 mg/μL, in order to get the mass concentration in mg/L. As *SMD* increased, a decreasing trend in the LISST *SSC* values was observed.

3.3. Correlations between SMD and granulometric percentiles (d_{50}, d_{10} and d_{90})

In fluvial and maritime hydraulics studies the median diameter, d_{50}, is mostly used as the characteristic diameter of the size distribution. Other diameters normally used are d_{10} and d_{90}. Empirical

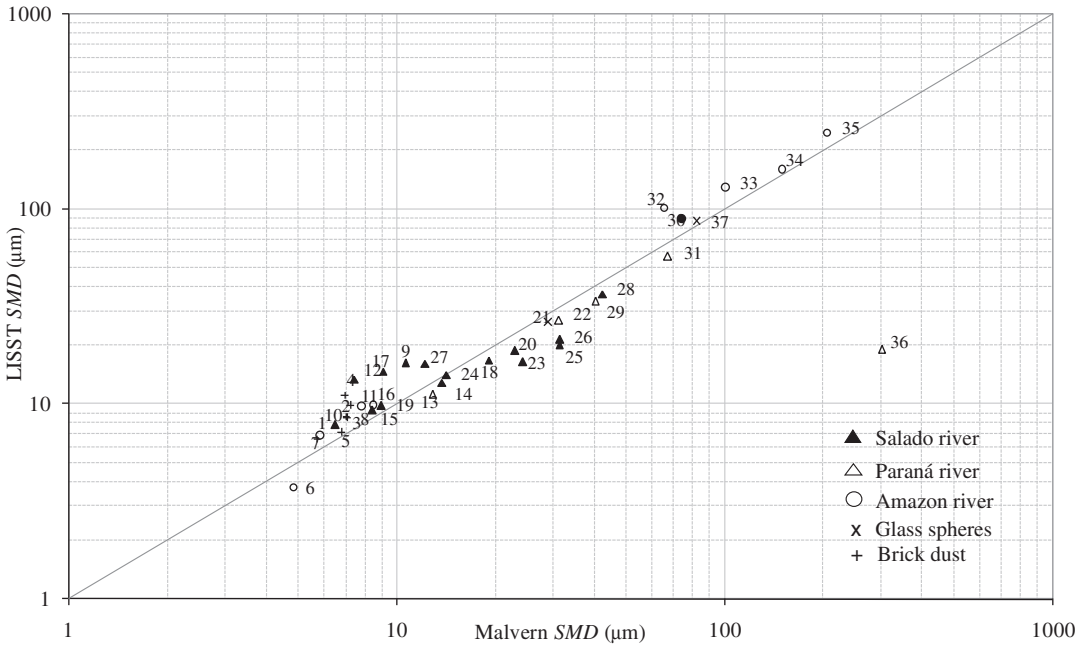

Fig. 4. *SMD* comparison: *SMD* measured with LISST and *SMD* obtained with Malvern. For samples tested with the two LISST models (B41, B58, E2 and E1), it is shown the *SMD* measured with model 1.

relationships between Malvern *SMD* and d_{50}, d_{10} and d_{90}, also measured with Malvern, were established and shown in Figs. 8, 9 and 10. The observed correlations between the *SMD* versus d_{50} and d_{10}, showed R^2 ~0.79 and 0.98, respectively. However for d_{90} a weak correlation was observed, resulting in R^2 being lower than 0.5.

Once the agreement between *SMD* measurements using LISST instruments and Malvern was verified, it was possible to use the former relationships, displayed in Figs. 8, 9 and 10, in order to estimate the percentiles of the size distribution from the *SMD* measured with LISST.

When the samples with bi-modal distributions, 15 of 37, are removed from the correlations above, the *SMD* vs d_{50} correlation improves, with an increase of R^2 from 0.79 to 0.86, *SMD* vs d_{10} correlation does not change, and *SMD* vs d_{90} correlation also improves with an increase of R^2 from 0.48 to 0.66.

4. Discussion

A high correlation was observed between LISST *SMD* and Malvern *SMD*, with a determination coefficient of $R^2 = 0.98$, in spite of the difference between the instruments and the experimental conditions. LISST 25X is a field instrument whereas Malvern is mostly used in

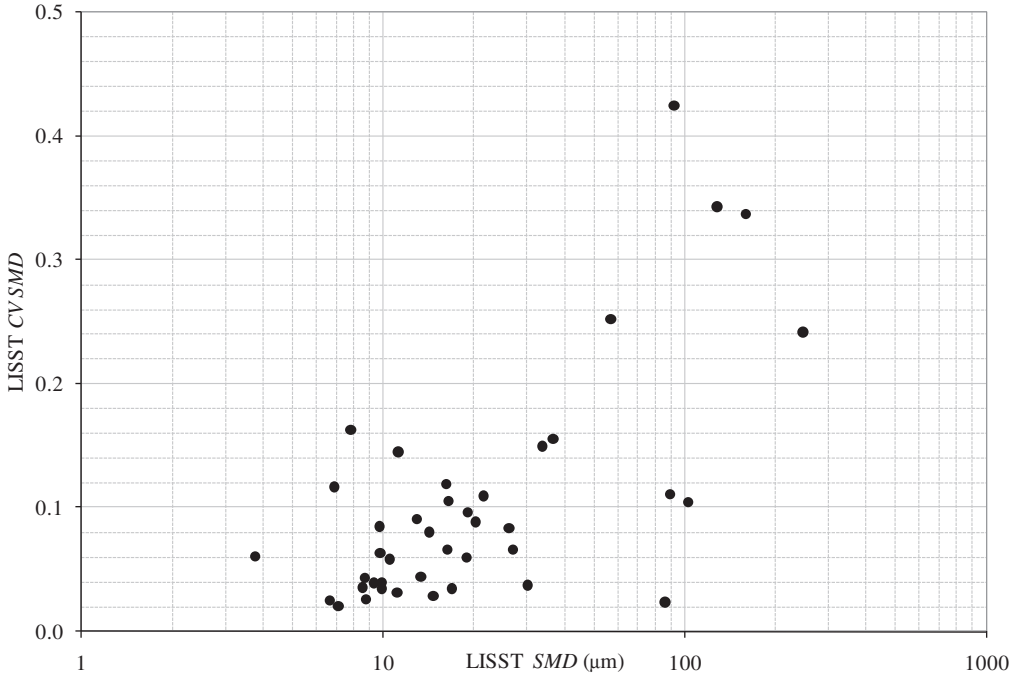

Fig. 5. Relationship between *SMD* (measured with LISST) vs *CV*.

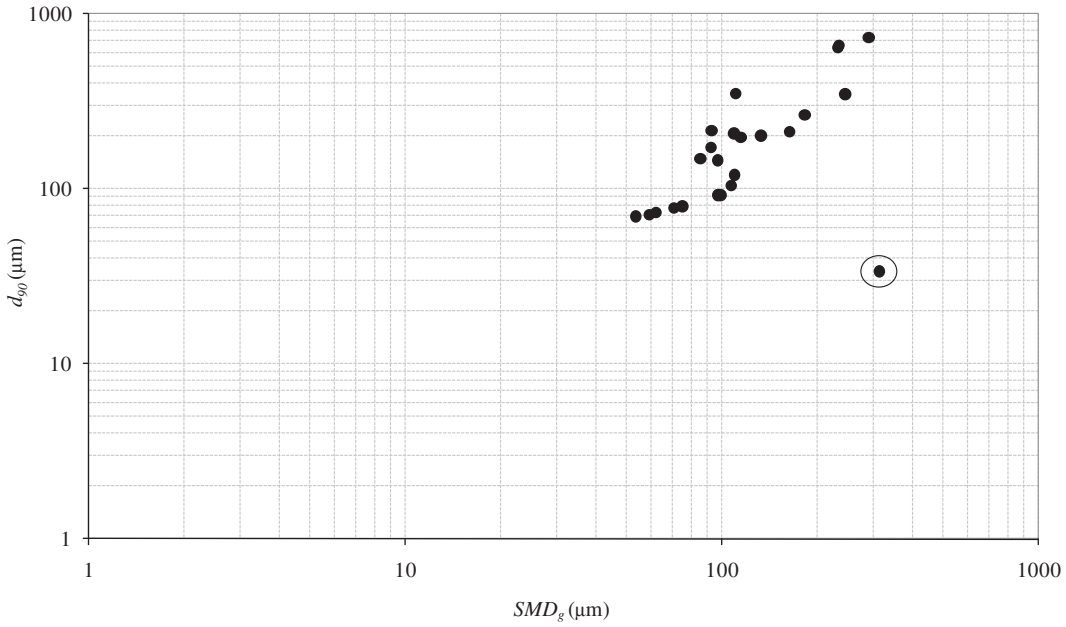

Fig. 6. Relationship between SMD_g (measured with LISST) and d_{90} (measured with Malvern).

laboratory work, and the size range measured by LISST runs from 2 to 500 μm and by Malvern from 0.02 to 2000 μm.

The tendency of LISST 25X to underestimate *SMD* in the coarser samples could be related to the agitation conditions of the water inside the test chamber as a result of the sedimentation of the coarser particles, or due to the reduced sampling volume. While Malvern pumps a considerable amount of sample through the sensor, LISST sample volume depends on the established sampling time and external agitation conditions. These sampling conditions were assessed through the variability coefficient, which in fact showed larger variability associated with the coarse samples ($CV>0.15$). The better mixture for finer sediments in the testing chamber would, therefore, generate less variability. However, high *CV* values were also detected for finer samples, such as AMP5H3G1, S19F, AMP5H3G4 and S36F (see Table 2). However in these cases, low uniformity ($d_{90}/d_{10}>10$) was observed, which may be attributed to the influence of the coarse fraction on the low sampling volume.

A large influence of the particle size in the LISST *SSC* was observed, decreasing *SSC* as the *SMD* increases (Fig. 7), which can be explained by resulting volume concentrations from surface measurements by optical instruments.

The available experimental conditions did not allow for testing the floc measurement capabilities. Floc size measurements are expected to be correctly determined by diffractometer instruments since the

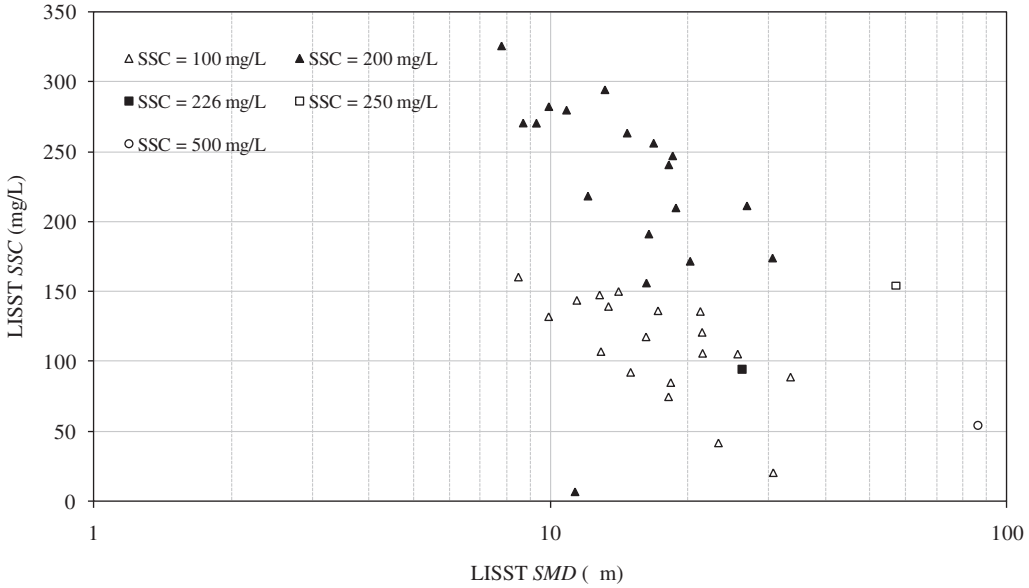

Fig. 7. Relationship between LISST *SSC* (measured with LISST model 1) and LISST *SMD* and actual *SSC*.

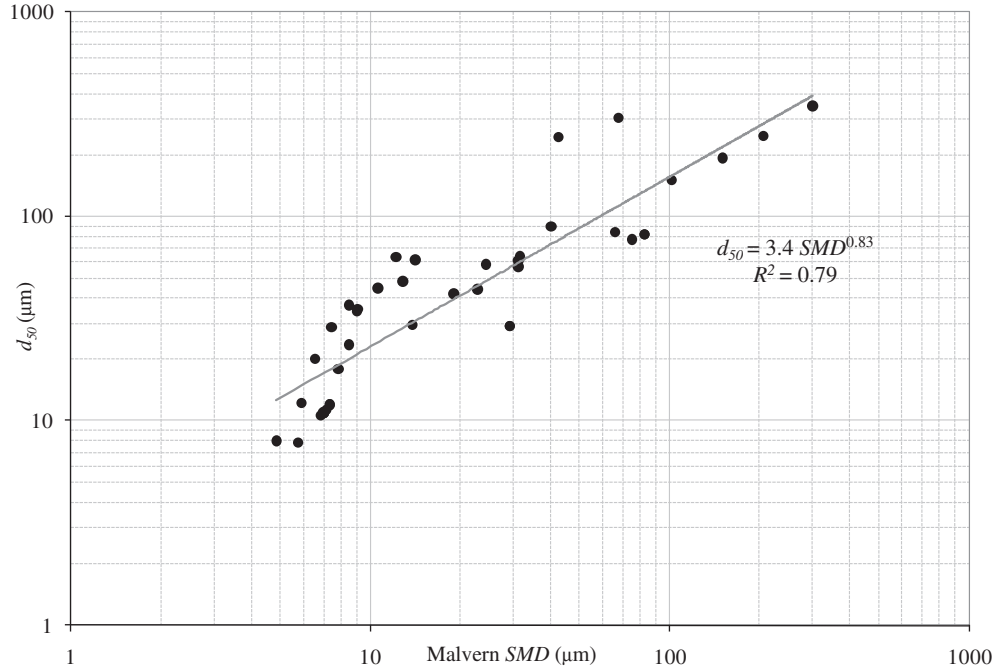

Fig. 8. Relationship between *SMD* and d_{50}, both measured with Malvern.

density of the particles will not interfere with the measurements. However, for suspended sediment concentration measurements, flocculation can be an extra factor limiting their usage.

5. Conclusions

The comparison between the *SMD* obtained with the LISST-25X (models 1 and 2) and the Malvern diffractometers showed that in samples bigger than 20 μm, the LISST instrument underestimated the values measured with the Malvern instrument; whereas, in samples smaller than 20 μm, the LISST instrument overestimated the values measured with the Malvern instrument. However, the relationship between the diffractometers was highly satisfactory, with a determination coefficient of $R^2 = 0.98$.

The observed results may indicate that where the mentioned sampling constraints do not appear, LISST-25X particle size measurements in natural water bodies improve. It is important to emphasize the need for following the recommended optical transmission, within the optimum levels: 30% to 98%, which can be restrictive for many natural environments.

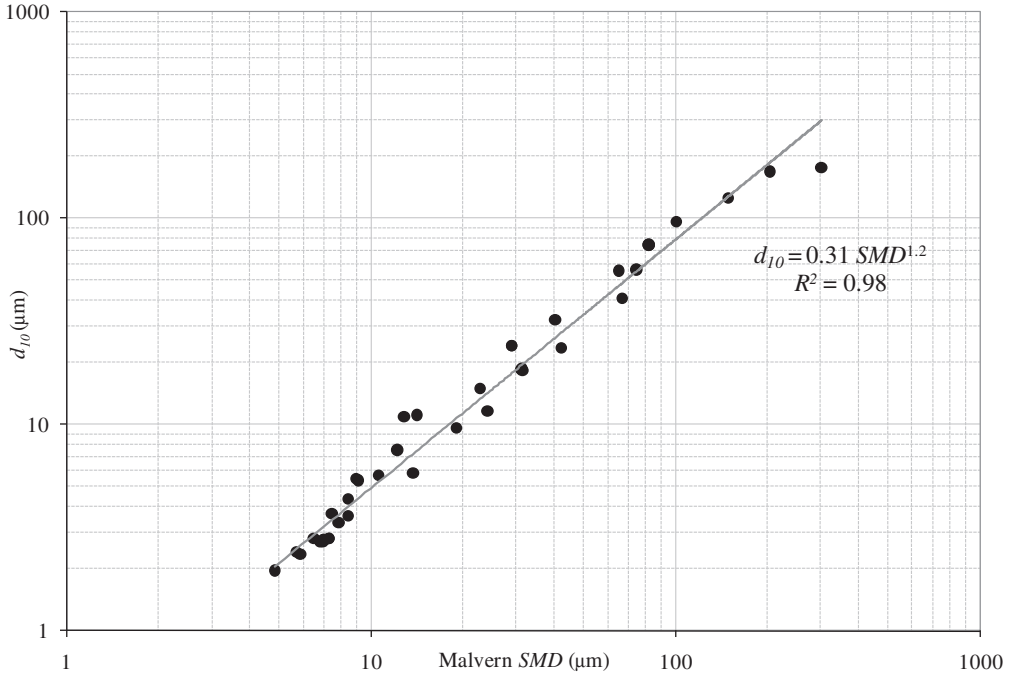

Fig. 9. Relationship between *SMD* and d_{10}, both measured with Malvern.

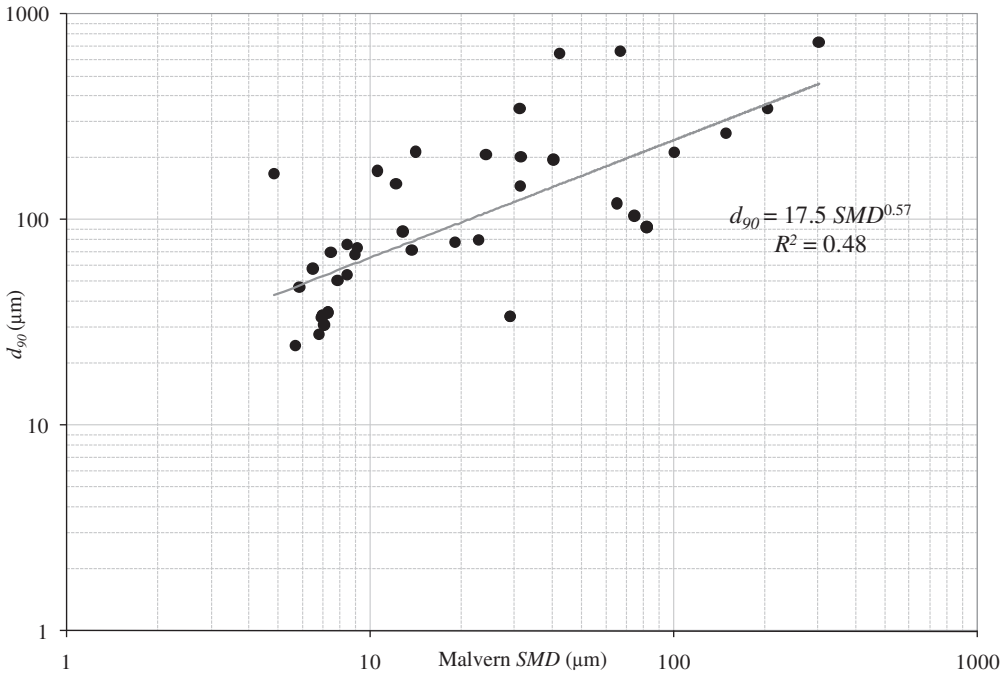

Fig. 10. Relationship between *SMD* and d_{90}, both measured with Malvern.

Satisfactory correlations were established between *SMD* and other characteristic diameters of the granulometric distribution, such as with d_{10}, d_{50} and d_{90}, all measured with Malvern. Therefore, it is possible to extend these correlations to the *SMD* obtained with LISST-25X and to use them to calculate the granulometric parameters of samples.

Acknowledgments

This work was supported by the Universidad Nacional del Litoral (UNL) and the Agencia Nacional de Promoción Científica y Tecnológica (ANPyCT) grant PICT 35885 to Dr. Alfredo Trento. Leonardo Filippa and Luana Freire receive PhD scholarships from ANPCyT, Agencia Nacional de Promoción Científica y Tecnológica, Argentina, and FAPERJ, Fundação de Amparo à Pesquisa do Estado do Rio de Janeiro, Brazil, respectively. Marcos Gallo is supported through the Pos-doc program PNPD/CAPES, Coordenação de Aperfeiçoamento de Pessoal de Nível Superior, Brazil. The authors are also grateful to the Laboratório de Geofísica Marinha (UERJ, Universidade Estadual do Rio de Janeiro, Brazil) for the use of the Malvern instrument.

References

Agrawal, Y.C., Mikkelsen, O.A., 2009. Shaped focal plane detectors for particle concentration and mean size observations. Optics Express, Optical Society of America 17, 23066–23077.

Agrawal, Y.C., Pottsmith, H.C., 1994. Laser diffraction particle sizing in STRESS. Continental Shelf Research 14, 1101–1112.

Agrawal, Y.C., Whitmire, A., Mikkelsen, O.A., Pottsmith, H.C., 2008. Light scattering by random shaped particles and consequences on measuring suspended sediments by laser diffraction. Journal of Geophysical Research 113, 1–11.

Dyer, K.R., Manning, A.J., 1999. Observation of the size, settling velocity and effective density of flocs, and their fractal dimensions. Journal of Sea Research 41, 87–95.

Eisma, D., Bale, A.J., Dearnaley, M.P., Fennessy, M.J. Van, Leussen, W., Maldiney, M.A., Pfeiffer, A., Wells, J.T., 1996. Intercomparison of in situ suspended matter (floc) size measurements. Journal of Sea Research 36 (1/2), 3–14.

Gartner, J., Cheng, R., Wang, P., Richter, K., 2001. Laboratory and field evaluations of the LISST-100 instrument for suspended particles size determinations. International Journal of Marine Geology, Geochemistry and Geophysics 175, 199–219.

Kumar, R.G., Strom, K.B., Keyvani, A., 2010. Floc properties and settling velocity of San Jacinto estuary mud under variable shear and salinity conditions. Continental Shelf Research 30, 2067–2081.

Lynch, J.F., Irish, J.D., Sherwood, C.R., Agrawal, Y.C., 1993. Determining suspended sediment particle size information from acoustical and optical backscatter measurements. Continental Shelf Research 14 (10/11), 1139–1165.

Manning, A. J., Mietta, F., & Winterwerp, J.C., 2009. An examination of the flocculation properties of natural cohesive sediment from the Scheldt estuary. In Proc. of 10th International Conference on Cohesive Sediment Transport Processes (INTERCOH 09). Río de Janeiro, Brasil.

Mietta, F., Chassagne, C., Winterwerp, J.C., 2009. Shear-induced flocculation of a suspension of kaolinite as function of pH and salt concentration. Journal of Colloid and Interface Science 336, 134–141.

Murray, D.M., Holtum, D.A., 1996. Inter-conversion of Malvern and sieve size distributions. Minerals Engineering 9 (12), 1263–1268.

Pacek, A.W., Man, C.C., Nienow, A.W., 1998. On the Sauter mean diameter and size distribution in turbulent liquid/liquid dispersions in a stirred vessel. Chemical Engineering Science 53, 2005–2011.

Rawle, A., 2010. Basic principles of particle size analysis. Technical report, <*http://www.malvern.com/malvern/kbase.nsf/allbyno/KB000021/$file/Basic_principles_of_particle_size_analysis_MRK034-low_res.pdf*>.

Sequoia, 2008. Operating principle of the LISST-25 constant calibration sediment sensor, <*http://sequoiasci.com/Articles*>.

Sequoia, 2009. LISST – 25 User's Guide, <*http://sequoiasci.com*>.

Shen, H.W., Julien, P.Y., 1993. Erosion and sediment transport. In: Maidment, D. (Ed.), Handbook of Hydrology. McGraw-Hill Inc.

Stramski, D., 2006. Parallel Measurements of Light Scattering and Characterization of Marine Particles in Water: An Evaluation of Methodology, http://www.mpl.ucsd.edu/people/stramski.

Topping, D., Wright, S. A., Melis, T. S., & Rubin, D. M., 2006. High resolution monitoring of suspended sediment concentration and grain size in the Colorado river using laser diffraction instruments and a three-frequency acoustic system. Final Proc. of 5th Symposium, Federal Interagency Sedimentation Comm., Reno, NV.

Traykovski, P., Latter, R., Irish, J., 1999. A laboratory evaluation of the laser in situ scattering and transmissometery instrument using natural sediments. International Journal of Marine Geology, Geochemistry and Geophysic 159, 355–367.